SCIENTIFIC REPORTS

OPEN

SUBJECT AREAS:
ULTRACOLD GASES
QUANTUM FLUIDS AND SOLIDS

Received
10 July 2014

Accepted
19 September 2014

Published
17 October 2014

Correspondence and requests for materials should be addressed to V.B.S. (shenoy@physics.iisc.ernet.in)

Cooling a Band Insulator with a Metal: Fermionic Superfluid in a Dimerized Holographic Lattice

Arijit Haldar & Vijay B. Shenoy

Center for Condensed Matter Theory, Department of Physics, Indian Institute of Science, Bangalore 560012, India.

A cold atomic realization of a quantum correlated state of many fermions on a lattice, eg. superfluid, has eluded experimental realization due to the entropy problem. Here we propose a route to realize such a state using holographic lattice and confining potentials. The potentials are designed to produces a *band insulating* state (low heat capacity) at the trap center, and a metallic state (high heat capacity) at the periphery. The metal "cools" the central band insulator by extracting out the excess entropy. The central band insulator can be turned into a superfluid by tuning an attractive interaction between the fermions. Crucially, the holographic lattice allows the emergent superfluid to have a *high transition temperature* – even twice that of the effective trap temperature. The scheme provides a promising route to a laboratory realization of a fermionic lattice superfluid, even while being adaptable to simulate other many body states.

Emulation of many body quantum systems[1,2] with cold atoms provides new opportunities to obtain answers to the most enigmatic problems of condensed matter physics[3] and even obtain phases with new topological order[4]. Notwithstanding the spectacular new developments[5–13], headway in the use of cold atomic systems to study interesting strongly interacting/correlated regimes such as those of the Hubbard model (both repulsive/attractive) has been hampered by the entropy problem[14]. For example, the remarkable progress made in the study of the BCS(Bardeen-Cooper-Schrieffer) to BEC(Bose-Einstein Condensate) of interacting fermions[15,16] (see[17] for an overview), has not been replicated on a lattice in the single band tight binding limit despite many proposals[18–25] (see also[14], and references therein).

The proposal in this paper, aimed at obtaining a fermionic superfluid in a lattice limit, contains two key ingredients. The first involves redistribution of entropy of the noninteracting cold gas in the trap such that, the trap-center carries very little entropy density, with the excess being "pushed out" to the peripheries of the trap. The second, the state at the center of the trap is chosen such that, upon tuning of interactions between the fermions, an interesting many body state, such as a superfluid, with a *high characteristic temperature* is realized.

Our scheme, which realizes both these ingredients simultaneously, uses a specially designed holographic optical lattice[10] along with an optical confining potential that obtains a *band insulator* state at the center of the trap, even while the periphery of the trap is in a gapless metallic state. Due to the high heat capacity of the metallic state, entropy flows from the center of the trap to the periphery, resulting in a band insulating center with a very low entropy density owing to its exponentially low heat capacity. The band insulator is thus cooled by the metal. On tuning an attractive interaction between opposite spin fermions, a superfluid state is realized from the band insulating state. Remarkably, by a suitable design of the holographic optical lattice (which is quite difficult in a conventional optical lattice with interfering lasers) the superfluid state can be rendered to have a high transition temperature. We show that parameters can be chosen such that the transition temperature can be as high as twice the effective trap temperature, promising a realistic route to the laboratory realization of a lattice superfluid (see fig. 1).

The proposed setup, a schematic of which is shown in fig. 2, uses a hologram H1 and a s-polarized laser beam (Beam 1) to generate the lattice potential. This is then superimposed on the confining potential generated by another hologram H2 from a secondary s-polarized beam source (Beam 2), using a beam splitter. Using two different sources with the same polarization ensures that the pattern intensities from both the holograms gets added without any interference, at the same time it keeps the polarization constant throughout the trap. The beams are suitably frequency detuned with respect to a hyperfine transition of the fermionic atoms. The axial confinement in the perpendicular direction (along the z axis) can be achieved either via a cross dipole trap[26] or by the use of evanescent waves[10]. Lattice potentials with optical holograms[10,27–31] have been used recently producing a

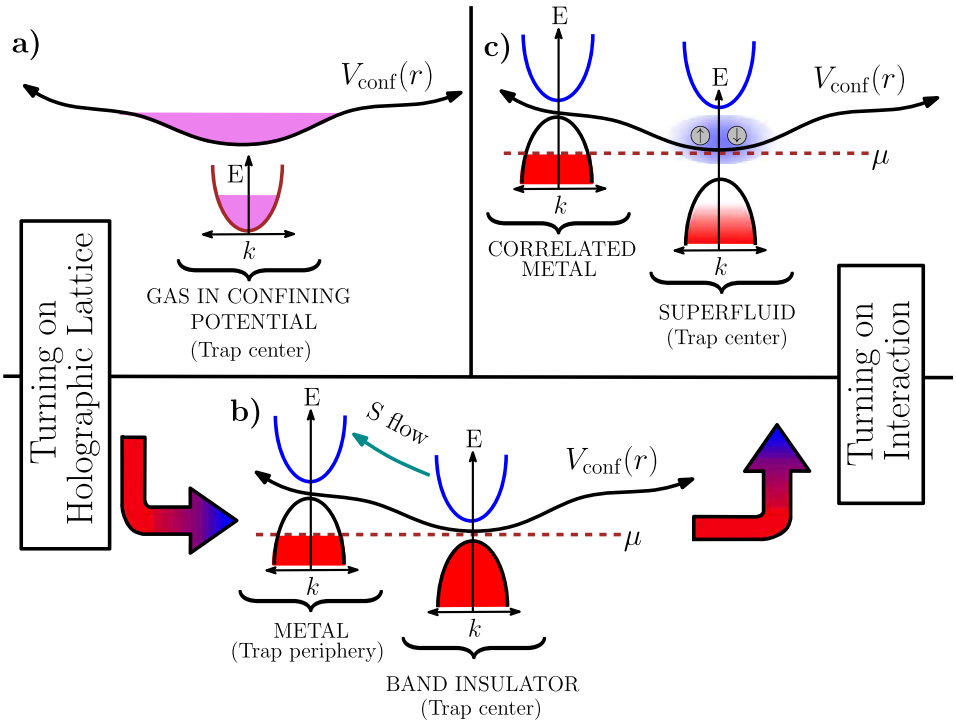

Figure 1 | Concept: (a) Stage 1: Fermion gas(with equal number of ↑ and ↓ spins) in a confining potential(V_{conf}) (without the lattice pattern); here fermion dispersion is qualitatively free particle like (purple curve).(b) Stage 2: The lattice pattern is adiabatically ramped up and superimposed on the existing confining potential, which results in a dispersion with conduction(blue) and valence(black) bands. The confining potential profile is designed to tune the local chemical potential such that the valence band is completely occupied near the trap center(band insulating state) and only partially occupied(metallic state) near the trap peripheries. This results in a flow of entropy(green arrow) from the center to the periphery; the metal "cools" the band insulator. The system around the trap center, in the band insulating state with one particle per site, has exponentially low entropy. (c) Stage 3: Adiabatically turning on attractive interaction causes the band insulator to form a high transition temperature superfluid by pairing of opposite spin fermions.

dazzling range of results in conjunction with the quantum gas microscope[10]. Holograms work by modulating the phase of the incident laser light spatially at every point of the beam cross-section. A given phase modulation pattern produces an intensity pattern that can then be scaled and focused by using suitable optical elements.

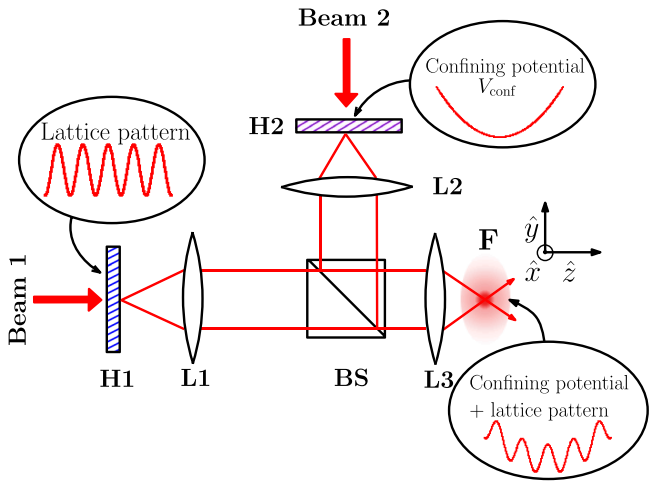

Figure 2 | **Proposed Setup: Hologram H1 modulates Beam 1, to encode the lattice pattern and hologram H2 encodes the confining potential into Beam 2.** Beam splitter(BS) combines the outputs from **H**1 and **H**2. Lenses L1–3 stand for the optics appropriate for obtaining the required potential at **F**.

Holograms such as these can be created permanently by lithographically etching a periodic mask into a dielectric substrate[10], or dynamically, by using a computer controlled spatial light modulator[29–32]. Robust algorithms are available[33–35] for calculating a phase modulation pattern to produce a target intensity profile.

The underlying plot in fig. 3(a) shows the profile of the optical lattice produced by the hologram **H**1 at **F**(see fig. 2). The potential consists of a double well (dimer) motif represented by the circles A and B, repeated periodically in space. The double well potential, which is a sum of two Gaussian potentials

$$V_{DW}(\vec{r}) = -V\left[\exp\left(-\frac{\left(x-\frac{a}{2}\right)^2}{w^2}\right) + \exp\left(-\frac{\left(x+\frac{a}{2}\right)^2}{w^2}\right)\right]\exp\left(-\frac{y^2}{w^2}\right), \quad (1)$$

is described by three parameters V (depth), w (width) and a (the spacing, see fig. 3(a)). We define $E_R = h^2/2ma^2$ which provides a kinetic energy scale, where m is the mass of the fermions. For a laser of wavelength 670 nm, $w \sim 270$ nm and $a \sim 900$ nm for $w/a = 0.3$. The double well is repeated periodically in space by basis vectors $\vec{a}_1 = (a + b\cos(\theta))\hat{x} + b\sin(\theta)\hat{y}$ and $\vec{a}_2 = (a + b\cos(\theta))\hat{x} - b\sin(\theta)\hat{y}$, where b and c are lengths and θ is an angle as shown in fig. 3(a). The resulting lattice potential is

$$V_{lat}(\vec{r}) = \sum_{\vec{R}_i} V_{DW}(\vec{r} - \vec{R}_i) \quad (2)$$

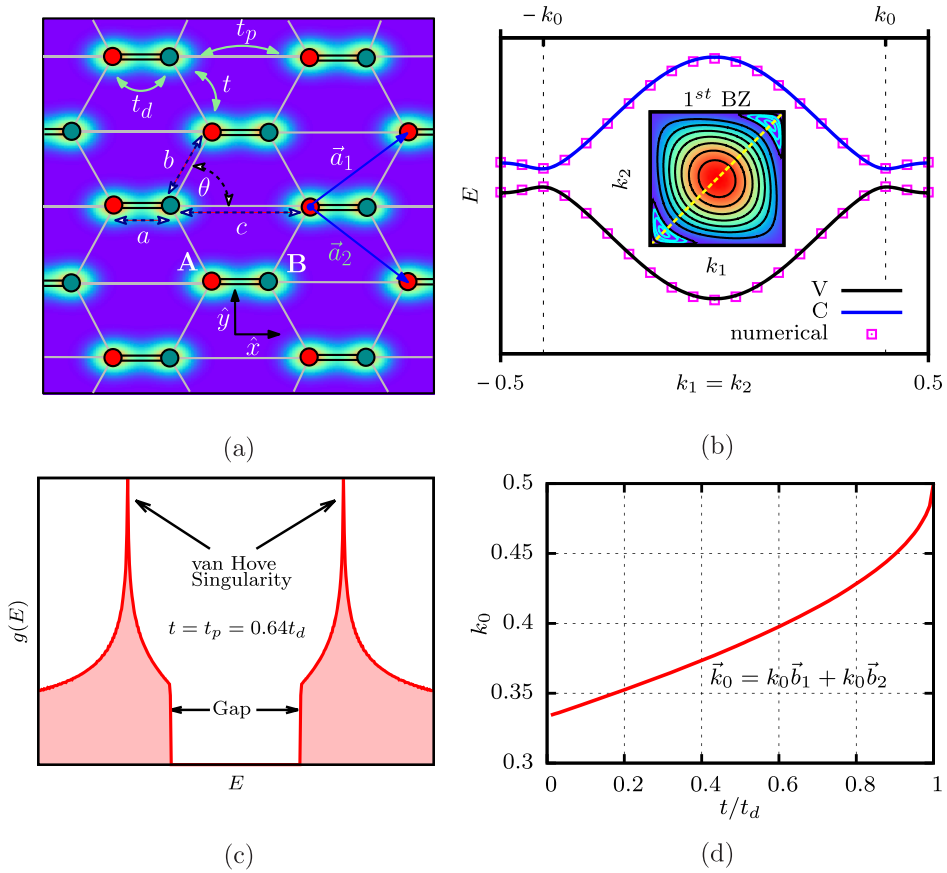

Figure 3 | Dimerized Holographic Lattice: (a) Lattice pattern of the dimerized holographic lattice with the tight binding model overlayed on top. Double lines are dimer bonds with hopping t_d. Single line slanted bonds have t and single line horizontal bonds have t_p hoppings. $\vec{a}_1$, $\vec{a}_2$ are lattice basis vectors. The distances a, b, c can be chosen by a suitable design of the hologram to obtain desired values of t/t_d and t_p/t_d. (b) Conduction(C) and valence(V) band dispersions showing the energy gap; blue(C) and black(V) bands correspond to that shown in fig. 1(b). The gap occurs at $\pm k_0$ along $k_1 = k_2$, as shown by the dashed line in the Brillouin zone plot(inset) of $\varepsilon_C - \varepsilon_V$ (see equation (3)). Holographic lattice parameter values are $V/E_R = 5.0$, $w/a = 0.3$ and $b/a = 1.04$. The area around $\pm k_0$ is highlighted with lighter contours. The resulting tight binding model has $t/t_d = t_p/t_d = 0.64$. (c) One particle density of states around the band gap, showing the van Hove singularities. (d) Dependence of wavevector k_0 (at which peaks in time-of-flight images are expected) on t/t_d. $\vec{b}_1$, $\vec{b}_2$ are reciprocal lattice vectors.

where $\vec{R}_i = n_1\vec{a}_1 + n_2\vec{a}_2$, where n_1, n_2 are integers. The significant advantage of using a hologram to generate this potential is that it allows greater freedom in the tuning of parameters b/a and c/a and θ. For a sufficiently deep lattice $V \gg E_R$, the low energy physics can be described by a tight binding model with the hopping parameters t_d (intra dimer), t and t_p (inter dimer). The flexibility in the design of the hologram allows us to choose $b = c$ as this obtains a superfluid with a high transition temperature (see below). This requires $\theta = \cos^{-1}\left[\frac{1}{2}\left(1-\frac{a}{b}\right)\right]$, making $t_p = t$.

For a given set of parameters (V, a, b etc.), we numerically solve for the Bloch states and their energy dispersion. By fitting the energy dispersion to a tight binding parametrization we obtain t_d, t and t_p; as expected, excellent fits are obtained in the deep lattice limit ($V \gg E_R$). The tight binding model allows for an analytical expression for the valance (V) and conduction (C) band dispersions:

$$\varepsilon_{V,C}\left(\vec{k}\right) = \mp\varepsilon\left(\vec{k}\right) = \mp\left[\left(t_d^2+3t^2\right)+2t^2\cos(2\pi(k_1-k_2))\right. \\ +2tt_d\cos(2\pi(k_1+k_2)) \\ \left.+2t(t_d+t)(\cos(2\pi k_1)+\cos(2\pi k_2))\right]^{\frac{1}{2}} \quad (3)$$

where $k_{1,2} \in [-1/2, 1/2]$, $\vec{k} = k_1\vec{b}_1 + k_2\vec{b}_2$, $\vec{b}_1$ and $\vec{b}_2$ are reciprocal lattice basis vectors. As is seen in fig. 3(b), the two bands are separated by a gap which occurs at two points in the Brillouin zone. For the parameters shown in fig. 3(b), the bands are nearly particle-hole symmetric. The density of states is finite at the band edges, but has a van Hove singularity inside the band (see fig. 3(c)). Fig. 3(d) shows the momentum k_0 (fig. 3(b)) where the direct band gap occurs. If the valance bands corresponding to both up and down spin fermions are filled, a band insulating state with one particle per site (two particles per unit cell) is obtained. It is this state that we exploit to obtain an optical lattice superfluid. This entails designing a confining potential that allows the realization of this band insulating state at the center of trap, and we now turn to the discussion of such a confining potential.

The choice of the in-plane confining potential plays a crucial role in the redistribution of entropy in the trap. Here we use an azimuthally symmetric trapping potential, encoded using the hologram **H2** (see, for example[34]) that has a form

$$V_{\text{conf}}(r) = V_h\left[1-\exp\left(-\frac{r^2}{l_h^2}\right)\right] \\ +\frac{V_d}{2}\left[\tanh(\gamma(r-r_d))+1\right] \quad (4)$$

where $r = \sqrt{x^2+y^2}$ is the radial coordinate. The potential (fig. 4(a)) has a central "harmonic region" where the band-insulating state is to be realized (in the region $0 \le r \le l_h$), a "slowly rising" region ($l_h \le r \le r_d$) which will hold the "metallic" state and a relatively sharp

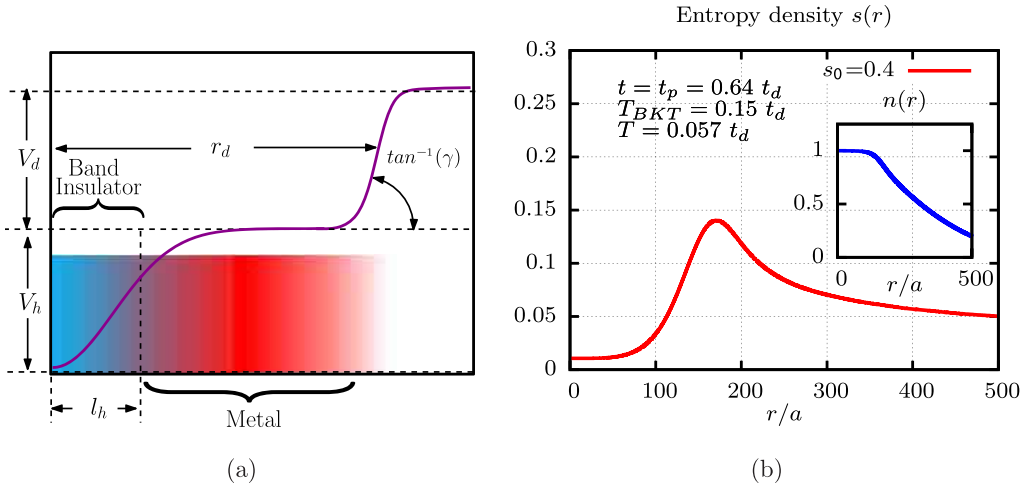

Figure 4 | Confining Potential: (a) Radial profile of the confining potential (see equation (4)). The lengths l_h and r_d can be tuned to adjust the relative size of band insulator and metallic regions. (b) Entropy density $s(r)$ and number density per site $n(r)$ (inset) plots, for $s_0 = 0.4$. The lattice potential considered corresponds to that discussed in fig. 3. The trap temperature $T/t_d \approx 0.057$. Confining potential parameters are $V_h/E_R = 0.0045$, $l_h/a = 450$, $r_d/a = 1700$.

upturn at $r = r_d$ (A simple harmonic trap is ill suited for this purpose since it holds relatively fewer atoms in the metallic state). Similar confining potentials have been considered in the literature[21].

The strategy now is to start from a cloud of cold gas with a given initial entropy per particle and load it into the confining potential as shown in fig. 1(a). The lattice potential is now adiabatically ramped up, and this will redistribute the particles and the entropy in the trap. The key point is that for suitably chosen parameters (which depends on the number of particles N_p, equal number of up and down spins), the central region of the trap will be in a band insulating state with a very low entropy density (owing to its exponentially small heat capacity). The outer metallic regions will be the "entropy dump" since it has a larger heat capacity (see fig. 1(b)). The final temperature of the system will be determined by total entropy and number balance.

We now estimate the final trap temperature and the entropy redistribution for a noninteracting system, keeping in mind that some interaction is, of course, necessary to equilibrate the system. The estimation proceeds through a local density approximation which begins with the definition of the local chemical potential $\mu_{\rm loc}(r) = \mu - V_{\rm conf}(r)$, ($\mu$ is the global chemical potential). The local number and entropy densities are

$$\rho(r,\ \mu_{\rm loc},\ T) = \int_{BZ} \frac{d^2\vec{k}}{2\pi^2} \sum_{b\in V,C} n_F\left(\frac{\varepsilon_b\left(\vec{k}\right) - \mu_{\rm loc}(r)}{T}\right)$$

$$s(r,\ \mu_{\rm loc},\ T) = -\int_{BZ} \frac{d^2\vec{k}}{2\pi^2} \sum_{b\in V,C} [n_F \ln(n_F) + (1-n_F)\ln(1-n_F)] \quad (5)$$

where n_F is the Fermi function. The two unknowns, i.e., the final temperature T and the global chemical potential μ are now obtained using

$$N_p = 2\pi \int_0^\infty dr\ r\ \rho(r,\ \mu_{\rm loc}(r), T)$$

$$S = 2\pi \int_0^\infty dr\ r\ s(r,\ \mu_{\rm loc}(r), T) \quad (6)$$

where $S = N_p s_0$, s_0 is the initial entropy per particle before ramping up the lattice potential.

We use the set of values mentioned in fig. 3(b), and adjust the confining potential parameters (V_h, l_h, r_d and γ), to obtain a low value of trap temperature, for a typical number of loaded atoms($N_p \approx 0.48 \times 10^6$) and entropy per particle($S/N_p \approx 0.6, 0.5, 0.4$). Fig. 4(b) shows the final entropy density in the trap as a function of the radial distance r for the lattice considered in fig. 3, with a starting entropy per particle, $s_0 = 0.4$. Both the entropy and number densities show a sizable core region which is in the band insulating state. It is heartening to note that the final trap temperature is less than a factor of two smaller than the temperature required to obtain superfluidity T_{BKT} (see below) in this band insulator. These calculations have assumed that the process of ramping of the lattice is adiabatic. To investigate if these encouraging results are spoiled by possible non-adiabatic effects; we can start with systems at even higher initial entropy s_0 to investigate how the trap temperature and central entropy vary. The results of Table I show that if the process of turning on the lattice is reasonably well controlled, then the additional entropy of this process will not be debilitating. We further show that the scheme is robust to changes in the particle number, in that a variation of N_p by $\pm 10\%$ results in trap temperatures(T) well below the superfluid transistion temperature($T_{\rm BKT}$).

Having obtained a low entropy band insulating state, we now tune an onsite attractive interaction U of the Hubbard type (using, e.g., a Feshbach resonance[36,37]) to drive the band insulating state into a superfluid state[25,38–43]. The emergent superfluid state can be modeled by the action

Table I | Trap temperature(T) and trap center entropy for various values of initial entropy per particle(s_0) and number of atoms(N_p) loaded into the trap($N_0 = 0.48 \times 10^6$). In all cases the final trap temperature(T) is well below the transisiton temperature($T_{BKT} = 0.15 t_d$) of the superfluid, for the parameters shown in fig. 3

$N_p = N_0$			$N_p = 0.9N_0$			$N_p = 1.1N_0$		
s_0	T trap	s center	s_0	T trap	s center	s_0	T trap	s center
0.4	$0.057t_d$	0.010	0.4	$0.066t_d$	0.023	0.4	$0.050t_d$	0.008
0.5	$0.073t_d$	0.027	0.5	$0.081t_d$	0.046	0.5	$0.066t_d$	0.021
0.6	$0.089t_d$	0.051	0.6	$0.097t_d$	0.075	0.6	$0.083t_d$	0.041

$$S = S_0 + S_U$$
$$S_0 = \int_0^{1/T} d\tau \sum_{\vec{k},\sigma} \sum_{\alpha\beta} c^*_{\vec{k}\alpha\sigma}(\tau) \left[\delta_{\alpha\beta} \frac{\partial}{\partial \tau} + \varepsilon_{\alpha\beta}\left(\vec{k}\right) \right] c_{\vec{k}\beta\sigma}(\tau)$$
$$S_U = -\frac{U}{N} \int_0^{1/T} d\tau \sum_{\alpha \vec{k}_1 \vec{k}_2 \vec{k}'_1 \vec{k}'_2} \delta_{\left(\vec{k}_1 + \vec{k}'_1 - \vec{k}_2 - \vec{k}'_2\right)} c^*_{\vec{k}_2 \alpha\uparrow}(\tau) c^*_{\vec{k}'_2 \alpha\downarrow}(\tau) c_{\vec{k}'_1 \alpha\downarrow}(\tau) c_{\vec{k}_1 \alpha\uparrow}(\tau) \quad (7)$$

where $c_{\vec{k}\alpha\sigma}(\tau)$ stands for the fermion Grassman variable associated with momentum $\vec{k}$, sublattice flavour α, $\beta = A, B$; σ is the spin label, τ is the imaginary time, N is the number of unit cells of the homogeneous system, and $\varepsilon_{\alpha\beta}\left(\vec{k}\right)$ is a 2×2 matrix, defined as

$$\begin{bmatrix} 0 & -t_d - t\, e^{-i\vec{k}\cdot\vec{a}_1} - t\, e^{-i\vec{k}\cdot\vec{a}_2} - t_p\, e^{-i\vec{k}\cdot(\vec{a}_1+\vec{a}_2)} \\ \text{c.c} & 0 \end{bmatrix}.$$

The eigenvalues of $\varepsilon_{\alpha\beta}\left(\vec{k}\right)$ are the bands $\varepsilon_{V,C}$(equation (3)), when $t = t_p$. We analyze the superfluid state and its transition temperature by introducing a Hubbard-Stratanovic pairing field Δ_α for each site-flavour and looking for a uniform saddle point solution. When the saddle point is non-zero, we consider Gaussian fluctuations about it and obtain the collective excitations of the superfluid which govern the transition temperature, owing to the 2D nature of our system. In the following we shall only discuss the final physics, see[25] for details.

Unlike in a system with a ground state Fermi surface, our band insulator does not undergo a pairing instability for an arbitrary small attractive interaction. In fact, a finite critical U_c,

$$\frac{1}{U_c} = \frac{1}{2N} \sum_{\vec{k}} \frac{1}{\left|\varepsilon\left(\vec{k}\right)\right|} \quad (8)$$

($\varepsilon\left(\vec{k}\right)$ defined in equation (3)) is required to drive the pairing instability. $U_c = 1.96 t_d$ for the case considered in fig. 3. If $U > U_c$, then the pairing instability sets in at a temperature T_P determined by

$$\frac{1}{U} = \frac{1}{2N} \sum_{\vec{k}} \frac{1}{\varepsilon\left(\vec{k}\right)} \tanh\left(\frac{\varepsilon\left(\vec{k}\right)}{2T_P}\right). \quad (9)$$

Even for $T < T_P$, superfluid long range order is discouraged by collective excitations of this system. Indeed, there exists a Beresinskii-Kosterlitz-Thouless temperature T_{BKT} below which a critical superfluid phase arises[44–46]. We calculate T_{BKT} by a study of the collective modes of the broken symmetry superfluid phase. In our system, owing to the presence of two sites per unit cell, there are four distinct collective modes. Two of these are gapped amplitude modes which do not enter the low energy physics. The other two are phase modes that correspond to phase fluctuations that are either in-phase between the two sites of the unit cell (symmetric phase mode), which is gapless, or out-of-phase (anti-symmetric mode, Leggett mode[47]), which is gapped. In our system these modes are coupled, and an effective superfluid stiffness ρ_{SF} tensor can be obtained by integrating out the amplitude modes and the Leggett mode. From this the critical temperature can be calculated as

$$T_{BKT} = \frac{\pi}{4} \mathrm{Tr}[\rho_{SF}]. \quad (10)$$

Interestingly, the temperature regime $T_{BKT} < T < T_P$ corresponds to a state with uncondensed fermion pairs displaying pseudogap like features[3]. For the system considered in fig. 3, we find that $T_P = 0.55 t_d$ and $T_{BKT} = 0.15 t_d$ (see fig. 5). We emphasize here that these large temperature scales are obtained by *design of the kinetic energy operator* which is encoded in the hologram **H1**. The superfluid stiffness which determines T_{BKT} is determined by the effective hoppings of the pairs which in turn is determined by the topology of the lattice. Here the holographic lattice allows the possibility to choose designs that maximize the superfluid stiffness, leading to the choice of $\theta = \cos^{-1}\left[\frac{1}{2}\left(1 - \frac{a}{b}\right)\right]$. The same idea is used to enhance the pairing scale T_P to produce a significant regime of pseudogap physics (see fig. 5) and simultaneously mitigate other uninteresting competing orders. For example, the large density of states near the band edges helps in enhancing T_P. Further, the gap in the one particle spectrum occurs at two lattice incommensurate k- vectors $\vec{k}_0$(see fig. 3(b,c)) which renders a competing state like a charge density wave unfavorable, particularly in a trap.

Having demonstrated a scheme that meets the two desiderata outlined earlier, viz. redistribution of entropy to create a low entropy state, and production of an interesting many body state with a high characteristic temperature by tuning an interaction in this state, we now turn to the detection of the high temperature superfluid phase realized. Pairing in this system takes place by promoting opposite spin particles from the valance band to the conduction band near momenta $\vec{k}_0$ (see fig. 3(b,c,d)). Pairing that occurs will therefore be evident in time of fight images where two peaks of equal intensity will appear at $\pm k_0$ corresponding to the states in the conduction band (with a concomitant dip in the states corresponding to the valance band). These can be separately detected using band mapping techniques[11,48,49]. Our proposal is particularly suited for detecting the superfluid phase by direct imaging in a quantum gas microscope[10]. It will also be quite interesting to explore the possibility of using methods like RF spectroscopy[50], photoemission spectroscopy[51] and spatially resolved Bragg spectroscopy[52] to detect superfluidity.

It is interesting to compare the present scheme with earlier works. The present proposal hinges on the concurrent use of two ideas namely (i) the creation of conditions such that the central region of the trap is a state with low characteristic entropy, and (ii) the design of a system that allows for an interesting quantum state (a fermionic superfluid) with high characteristic temperature to emerge at the trap centre, upon tuning of an interaction. Our proposal achieves the first goal by using a "metallic" state at the periphery of the trap to cool the band insulating state at the centre of the trap. This can be effectively viewed as, using the terminology of

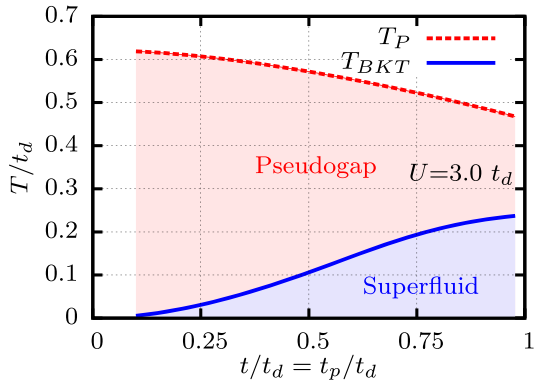

Figure 5 | Temperature Regimes of the Band Insulator Superfluid: Plot of T_P (dashed red line), the temperature below which pairing of fermions is favored and T_{BKT} (solid blue line), the Beresinskii-Kosterlitz-Thouless temperature below which superfluidity emerges, as a function of t/t_d, for $U/t_d = 3.0$.

ref. 14, a combination of "spatial filtering"[21,22,53] and "immersion cooling"[20,54–57] used simultaneously. The metallic regions being in the periphery of the trap achieves spatial filtering; alternately, this can also be viewed as immersion cooling achieved by placing the band insulating region in contact with a metallic bath which sucks up the entropy. A crucial new aspect of our proposal is the use of a holographic lattice to produce a band insulating state in the tight binding limit with an occupancy of one particle per site. This state allows the realization of the second key ingredient, i. e., a superfluid state with a high transition temperature. The key advantage of the present proposal is that two ideas (i) and (ii) stated above are achieved simultaneously in our system. Indeed, while the conceptual demonstration of our proposal provides encouraging results, the scheme clearly can be further optimized for an actual laboratory realization, providing a route to the long awaited lattice fermionic superfluid in a cold atomic system.

A.H. thanks CSIR, and V.B.S. is grateful to DST and DAE for financial support. The authors are grateful to Tilman Esslinger for discussions regarding experimental realization of the proposal.

1. Cirac, J. I. & Zoller, P. Goals and opportunities in quantum simulation. *Nat. Phys.* **8**, 264 (2012).
2. Trabesinger, A. Quantum simulation. *Nat. Phys.* **8**, 263 (2012).
3. Lee, P. A., Nagaosa, N. & Wen, X.-G. Doping a mott insulator: Physics of high-temperature superconductivity. *Rev. Mod. Phys.* **78**, 17 (2006).
4. Nayak, C., Simon, S. H., Stern, A., Freedman, M. & Das Sarma, S. Non-abelian anyons and topological quantum computation. *Rev. Mod. Phys.* **80**, 1083 (2008).
5. Lin, Y.-J. *et al.* Bose-einstein condensate in a uniform light-induced vector potential. *Phys. Rev. Lett.* **102**, 130401 (2009).
6. Lin, Y.-J., Compton, R. L., Jimenez-Garcia, K., Porto, J. V. & Spielman, I. B. Synthetic magnetic fields for ultracold neutral atoms. *Nature* **462**, 628 (2009).
7. Lin, Y.-J., Jimenez-Garcia, K. & Spielman, I. B. Spin-orbit-coupled bose-einstein condensates. *Nature* **471**, 83 (2011).
8. Cheuk, L. W. *et al.* Spin-injection spectroscopy of a spin-orbit coupled fermi gas. *Phys. Rev. Lett.* **109**, 095302 (2012).
9. Wang, P. *et al.* Spin-orbit coupled degenerate fermi gases. *Phys. Rev. Lett.* **109**, 095301 (2012).
10. Bakr, W. S., Gillen, J. I., Peng, A., Fölling, S. & Greiner, M. A quantum gas microscope for detecting single atoms in a hubbard-regime optical lattice. *Nature* **462**, 74 (2009).
11. Tarruell, L., Greif, D., Uehlinger, T., Jotzu, G. & Esslinger, T. Creating, moving and merging dirac points with a fermi gas in a tunable honeycomb lattice. *Nature* **483**, 302 (2012).
12. Aidelsburger, M. *et al.* Realization of the hofstadter hamiltonian with ultracold atoms in optical lattices. *Phys. Rev. Lett.* **111**, 185301 (2013).
13. Miyake, H., Siviloglou, G. A., Kennedy, C. J., Burton, W. C. & Ketterle, W. Realizing the harper hamiltonian with laser-assisted tunneling in optical lattices. *Phys. Rev. Lett.* **111**, 185302 (2013).
14. McKay, D. C. & DeMarco, B. Cooling in strongly correlated optical lattices: prospects and challenges. *Rep. Prog. Phys.* **74**, 054401 (2011).
15. Eagles, D. M. Possible pairing without superconductivity at low carrier concentrations in bulk and thin-film superconducting semiconductors. *Phys. Rev.* **186**, 456 (1969).
16. Leggett, A. J. *Modern Trends in the Theory of Condensed Matter,* [Pekalski, A. & Przystawa, R.] (Springer-Verlag, Berlin, 1980).
17. [The BCS-BEC Crossover and the Unitary Fermi Gas] *Lecture Notes in Physics* vol. **836** [Zwerger, W.] (Springer-Verlag, Berlin, 2012).
18. Ho, T.-L. The intrinsic difficulties of constructing strongly correlated states of lattice quantum gases by connecting up pre-engineered isolated atomic clusters. *arXiv: 0808.2677* (2008).
19. Capogrosso-Sansone, B., Söyler, S. G., Prokof'ev, N. & Svistunov, B. Monte carlo study of the two-dimensional bose-hubbard model. *Phys. Rev. A* **77**, 015602 (2008).
20. Ho, T.-L. & Zhou, Q. Squeezing out the entropy of fermions in optical lattices. *Proc. Natl. Acad. Sci. USA* **106**, 6916 (2009).
21. Ho, T.-L. & Zhou, Q. Universal Cooling Scheme for Quantum Simulation. *ArXiv e-prints* (2009), 0911.5506.
22. Bernier, J.-S. *et al.* Cooling fermionic atoms in optical lattices by shaping the confinement. *Phys. Rev. A* **79**, 061601 (2009).
23. Paiva, T., Loh, Y. L., Randeria, M., Scalettar, R. T. & Trivedi, N. Fermions in 3d optical lattices: Cooling protocol to obtain antiferromagnetism. *Phys. Rev. Lett.* **107**, 086401 (2011).
24. Tang, B., Paiva, T., Khatami, E. & Rigol, M. Finite-temperature properties of strongly correlated fermions in the honeycomb lattice. *Phys. Rev. B* **88**, 125127 (2013).
25. Prasad, Y., Medhi, A. & Shenoy, V. B. Fermionic superfluid from a bilayer band insulator in an optical lattice. *Phys. Rev. A* **89**, 043605 (2014).
26. Gemelke, N., Zhang, X., Hung, C.-L. & Chin, C. In situ observation of incompressible mott-insulating domains in ultracold atomic gases. *Nature* **460**, 995 (2009).
27. Boyer, V. *et al.* Dynamic manipulation of bose-einstein condensates with a spatial light modulator. *Phys. Rev. A* **73**, 031402 (2006).
28. Bergamini, S. *et al.* Holographic generation of microtrap arrays for single atoms by use of a programmable phase modulator. *JOSA B* **21**, 1889 (2004).
29. McGloin, D., Spalding, G., Melville, H., Sibbett, W. & Dholakia, K. Applications of spatial light modulators in atom optics. *Opt. Express* **11**, 158 (2003).
30. Gaunt, A. L. & Hadzibabic, Z. Robust digital holography for ultracold atom trapping. *Sci. Rep.* **2** (2012).
31. He, X., Xu, P., Wang, J. & Zhan, M. Rotating single atoms in a ring lattice generated by a spatial light modulator. *Opt. Express* **17**, 21007 (2009).
32. Hazlett, E. L., Ha, L.-C., Clark, L. W., Eismann, U. & Chin, C. Creation of arbitrary optical potentials for an atomic quantum gas. *Bull. Am. Phys. Soc.* **58** (2013).
33. Pasienski, M. & DeMarco, B. A high-accuracy algorithm for designing arbitrary holographic atom traps. *Opt. Express* **16**, 2176 (2008).
34. Liang, J., Kohn Jr, R. N., Becker, M. F. & Heinzen, D. J. *et al.* 1.5% root-mean-square flat-intensity laser beam formed using a binary-amplitude spatial light modulator. *Appl. Opt.* **48**, 1955 (2009).
35. Wyrowski, F. & Bryngdahl, O. Iterative fourier-transform algorithm applied to computer holography. *JOSA A* **5**, 1058 (1988).
36. Chin, C., Grimm, R., Julienne, P. & Tiesinga, E. Feshbach resonances in ultracold gases. *Rev. Mod. Phys.* **82**, 1225 (2010).
37. Diener, R. B. & Ho, T.-L. Fermions in optical lattices swept across feshbach resonances. *Phys. Rev. Lett.* **96**, 010402 (2006).
38. Moon, E. G., Nikolić, P. & Sachdev, S. Superfluid-insulator transitions of the fermi gas with near-unitary interactions in a periodic potential. *Phys. Rev. Lett.* **99**, 230403 (2007).
39. Zhai, H. & Ho, T.-L. Superfluid-insulator transition of strongly interacting fermi gases in optical lattices. *Phys. Rev. Lett.* **99**, 100402 (2007).
40. Fujihara, Y., Koga, A. & Kawakami, N. Superfluid properties of ultracold fermionic atoms in two-dimensional optical lattices. *Phys. Rev. A* **81**, 063627 (2010).
41. Diener, R. B., Sensarma, R. & Randeria, M. Quantum fluctuations in the superfluid state of the bcs-bec crossover. *Phys. Rev. A* **77**, 023626 (2008).
42. Burkov, A. A. & Paramekanti, A. Multiband superfluidity and superfluid to band-insulator transition of strongly interacting fermionic atoms in an optical lattice. *Phys. Rev. A* **79**, 043626 (2009).
43. Nikolić, P., Burkov, A. A. & Paramekanti, A. Finite momentum pairing instability of band insulators with multiple bands. *Phys. Rev. B* **81**, 012504 (2010).
44. Minnhagen, P. The two-dimensional coulomb gas, vortex unbinding, and superfluid-superconducting films. *Rev. Mod. Phys.* **59**, 1001 (1987).
45. Dupuis, N. Berezinskii-kosterlitz-thouless transition and bcs-bose crossover in the two-dimensional attractive hubbard model. *Phys. Rev. B* **70**, 134502 (2004).
46. Hadzibabic, Z., Krüger, P., Cheneau, M., Battelier, B. & Dalibard, J. Berezinskii–kosterlitz–thouless crossover in a trapped atomic gas. *Nature* **441**, 1118 (2006).
47. Leggett, A. J. Number-phase fluctuations in two-band superconductors. *Prog. Theor. Phys.* **36**, 901 (1966).
48. Trotzky, S. *et al.* Time-resolved observation and control of superexchange interactions with ultracold atoms in optical lattices. *Science* **319**, 295 (2008).
49. Bloch, I., Dalibard, J. & Zwerger, W. Many-body physics with ultracold gases. *Rev. Mod. Phys.* **80**, 885 (2008).
50. Chin, C. *et al.* Observation of the pairing gap in a strongly interacting fermi gas. *Science* **305**, 1128 (2004).
51. Stewart, J., Gaebler, J. & Jin, D. Using photoemission spectroscopy to probe a strongly interacting fermi gas. *Nature* **454**, 744 (2008).
52. Lingham, M., Fenech, K., Hoinka, S. & Vale, C. Local observation of pair condensation in a fermi gas at unitarity. *Phys. Rev. Lett.* **112**, 100404 (2014).
53. Sørensen, A. S. *et al.* Adiabatic preparation of many-body states in optical lattices. *Phys. Rev. A* **81**, 061603 (2010).
54. Catani, J. *et al.* Entropy exchange in a mixture of ultracold atoms. *Phys. Rev. Lett.* **103**, 140401 (2009).
55. McKay, D. & DeMarco, B. Thermometry with spin-dependent lattices. *New J. Phys.* **12**, 055013 (2010).
56. Sørensen, O. S., Nygaard, N. & Blakie, P. Adiabatic cooling of a tunable bose-fermi mixture in an optical lattice. *Phys. Rev. A* **79**, 063615 (2009).
57. Brown-Hayes, M., Wei, Q., Presilla, C. & Onofrio, R. Thermodynamical approaches to efficient sympathetic cooling in ultracold fermi-bose atomic mixtures. *Phys. Rev. A* **78**, 013617 (2008).

Acknowledgments

A.H. thanks CSIR, and V.B.S. is grateful to DST and DAE for financial support. The authors are grateful to Tilman Esslinger for discussions regarding experimental realization of the proposal.

Author Contribution

A.H. and V.B.S. contributed to the work and preparation of the manuscript.

Additional information

Competing financial interests: The authors declare no competing financial interests.

How to cite this article: Haldar, A. & Shenoy, V.B. Cooling a Band Insulator with a Metal: Fermionic Superfluid in a Dimerized Holographic Lattice. *Sci. Rep.* **4**, 6655; DOI:10.1038/srep06655 (2014).